Relationship between chemical and mechanical degradation of aged paper: fibre versus fibre–fibre bonds

Caroline Vibert, Anne-Laurence Dupont, Justin Dirrenberger, Raphaël Passas, Denise Ricard, Bruno Fayolle

Relationship between chemical and mechanical degradation of aged paper: fibre versus fibre-fibre bonds

https://doi.org/10.1007/s10570-023-05683-x

Authors: Caroline Vibert [a,b,c] * (https://orcid.org/0000-0002-7673-5260), Anne-Laurence Dupont [a] (https://orcid.org/0000-0003-0341-4850), Justin Dirrenberger [b] (https://orcid.org/0000-0002-3964-305X), Raphaël Passas [d] (https://orcid.org/0000-0002-2157-9846), Denise Ricard [c], Bruno Fayolle [b] * (https://orcid.org/0000-0002-9578-1692)

[a] Centre de Recherche sur la Conservation des Collections (CRC, CNRS UAR 3224), Muséum National d'Histoire Naturelle, 36 rue Geoffroy St Hilaire, 75005 Paris, France

[b] Laboratoire PIMM, Arts et Métiers Institute of Technology, CNRS, CNAM, HESAM Université, 151 boulevard de l'Hôpital, 75013 Paris, France

[c] ANDRA, French National Radioactive Waste Management Agency, F-92298 Châtenay-Malabry, France

[d] Laboratory of Process Engineering for Biorefinery, Bio-based Materials and Functional Printing, UMR CNRS 5518, Grenoble INP-Pagora, 461 rue de la papeterie, 38402 Saint-Martin-d'Hères, France

*Corresponding authors: caroline.m.vibert@gmail.com; bruno.fayolle@ensam.eu.

Abstract Paper is susceptible to chemical degradation through hydrolysis and oxidation, resulting in embrittlement and failure. Understanding the embrittlement process is important to ensure the preservation and longevity of historical paper-based documents. However, the complex and architectured paper microstructure is a major challenge for fully understanding this process. Two papers with different microstructures were artificially aged under hydrolytic and oxidative exposure conditions, and the consequences of ageing were studied. The fibre embrittlement, the fibre-fibre bonds deterioration, and the evolution of paper microstructure upon ageing are evaluated through macroscopic and localised mechanical tests, as well as through morphological observations at the microscopic scale. It was concluded, from the different tests in the two principal orientations of the paper, that fibre embrittlement plays a more significant role in the embrittlement process than fibre-fibre bonds deterioration.

Published online 05 January 2024

Specifically, the cellulose chain scissions led to fibre embrittlement, irrespective of the oxidative or hydrolytic nature of the chemical degradation mechanism. Furthermore, we identify a critical degree of polymerisation for cellulose (DP_c ~750) below which the evolution of mechanical properties accelerates significantly, regardless of the type of mechanical testing performed. Fibre analysis suggests that the decline in fibre resistance results in fractures occurring under stress at weak points of the fibres, such as kinks or twists.

Keywords Hydrolysis, Oxidation, Microstructure, Morphology, Tensile testing, Fibre orientation.

1 Introduction

Paper embrittlement is a major concern for the preservation of books and documents. Among the various aspects of paper ageing, mechanical resistance is of prime importance because it can seriously impede handling and reading. To address this issue, papers can be treated via a polymer network reinforcement, or lined on a more resistant paper substrate (Piovesan et al. 2018; Ferrandin-Schoffel et al. 2023). Permanent paper, which contains an alkaline reserve to slow down its ageing, can be used for long-term preservation and archival purposes (Frase 1997). However, understanding the consequences of degradation on the mechanical behaviour of paper, and more specifically the role of the fibres and fibre-fibre bonds in the embrittlement process, can help to better formulate the papers and the treatments with the aim of improving durability. The objective of this study is to provide further insight into the correlation between chemical and mechanical ageing of paper, in order to understand how the chemical degradation under different ageing conditions affects its mechanical properties. In this regard, two papers with different microstructures were studied.

Paper is a structured material made from plant fibres, usually from wood, bast fibres plants or cotton. During the manufacturing process, the fibres are separated from each other by chemical and mechanical treatments, suspended in water, then dried in the shape of sheets (Young and Rowell 1986; Neimo 1999). The papermaking machine induces an orientation of the fibres in the sheet, conferring to the paper an anisotropic mechanical behaviour. The fibres are entangled and adhere to each other through fibre-fibre bonds. These bonds consist on different adhesion phenomena: weak bonds such as Coulomb forces, Van der Waals forces and hydrogen bonds, and molecular interdiffusion between the swollen fibres in contact, mechanical entanglement of the fibrils on the surface of the fibres (Hirn and Schennach 2015). These fibrils are produced by the refining process in order to increase the contact surface and the mechanical entanglement, and therefore the adhesion between fibres (Sampson and Wang 2020). Moreover, the manufacturing process can induce defects along the fibre, such as kinks, or twists (Aslan et al. 2011; Ali 2012; Ciesielski et al. 2019; Richely et al. 2022). The characteristics of the fibres, including their

Published online 05 January 2024

nature, length and diameter, as well as the density of the sheets and the degree of refining are parameters that can vary from one paper to another, and that can have a strong impact on the mechanical properties (Iribarne and Schroeder 2000; l'Anson et al. 2006; Kontturi et al. 2021). These parameters should be monitored in order to reveal the relevant physical parameters that govern the changes in the mechanical behaviour upon chemical degradation.

Paper also contains other plant fibre structures, especially fibres' fragments of small size called fines, defined as the fraction of the pulp stock that will pass a round hole 76 µm in diameter (TAPPI standard method T 261 cm-00). They will be considered in this study, as they can have an impact on the mechanical strength of paper. Printing paper also contains additives, such as fillers and surface treatment products (Henniges et al. 2016),that can also impact mechanical behaviour.

However, the mechanical strength of paper is mostly determined by its structure, e.g., a random network of entangled fibres. The density of the network is responsible for contacts between fibres (Sampson 2001, 2009). They adhere to each other through deformable fibre-fibre bond (Iribarne and Schroeder 2000; Barbier et al. 2009) thanks to the phenomena described hereabove. The mechanical properties of paper are thus due to the strength of individual fibres, of fibre-fibre bonds, and to the entanglement between fibres.

Macroscopic mechanical properties can be obtained through tests such as compression, tensile tests or fatigue tests, which give information on the visco-elastoplastic behaviour of paper with damage (Haslach, Jr. 2000). Due to the orientation of the fibres in the sheet, these properties are determined in the two principal axes of the sheet (Kurei et al. 2022). However, to have access to the strength of individual fibres and fibre-fibre bonds, specific tests can be used, as for example tensile tests on unique fibres or adhesion tests on unique fibre-fibre bonds (Schmied et al. 2012; Yue et al. 2019; Maraghechi et al. 2023). Obtaining individual fibres behaviour is challenging, especially because papers include a wide range of fibres dimensions. Moreover, it may not accurately mirror the actual stress within a paper under tensile test. Therefore, i*n-situ* characterisation is necessary, and localised tests can be used. For example, the zero-span tensile test consists of pulling a paper strip with no gap between the jaws. It is considered that the pulling is exerted only on the fibres without loading the network (Gurnagul and Page 1989; Wathén et al. 2005; Batchelor et al. 2006). Similarly, water-saturated tensile test involves immersing the paper in water prior to testing, which results in the weakening of fibre-fibre bonds and favours fibre slippage.

Another approach consists in varying the structural parameters of paper and measure their impact on macroscopic properties to determine the contributions of fibre and fibre-fibre bonds resistance on the mechanical strength of

Published online 05 January 2024

paper (Marulier et al. 2015; Deogekar et al. 2019). Authors have studied the morphology of fibres by cutting them before the papermaking process, as well as the strength of bonding through refining or adjoining additives to the pulp (l'Anson et al. 2006). The impact of fibres morphology has been correlated to the mechanical properties in a semi-empirical equation introduced by Page (Page 1969) (**equation 1**). In particular, this equation links tensile and zero-span tensile strength to the length of fibres and to the bonding areas. Such microstructure parameters can be obtained through microscopic observations or X-ray microtomography (Peyrega et al. 2009; Bache-Wiig and Henden 2010; Wernersson et al. 2014; Emerson et al. 2017). However, quantification from such images can be difficult due to insufficient resolution leading to incomplete fibre identification, especially for dense papers. The wide range of available tests and their limitations highlight the need for a comprehensive study at the different length scales.

Cellulose being the main polymer that composes paper fibres, its degree of polymerisation (DP) is a key parameter to be monitored during the ageing of paper. The chemical degradation under archival conservation conditions is mainly due to the hydrolysis of cellulose (Gehlen 2010; SriBala and Vinu 2014). However, for permanent papers, the kinetics of the acid-catalysed hydrolysis being slowed down by an alkaline reserve, the oxidation of cellulose cannot be neglected (Nevell and Zeronian 1985; Margutti et al. 2001; Potthast et al. 2006). These two degradation mechanisms have several impacts on paper, including cellulose chain scissions and a change in cellulose crystallinity, consequently affecting paper water content (Haas et al. 1967; Gehlen 2010; Driemeier et al. 2012).

In the literature, the impact of chemical ageing on the mechanical strength of paper has been evaluated mostly through tensile and zero-span tensile tests (dry and wet) and folding endurance tests (Emsley et al. 1997; Zervos and Moropoulou 2005; Carrascal et al. 2018; Kurei et al. 2022). A significant reduction in folding endurance as well as an embrittlement of paper is observed in both artificially and naturally aged paper (Wilson et al. 1955; Barrow and Sproull 1959; Horst et al. 2020). Based on Page's equation, Zou concluded that acid cotton paper embrittlement under accelerated ageing was due to a decrease of fibre strength (Zou et al. 1994). Kaminska demonstrated that the relationship between the number of cellulose chain scissions and the zero-span breaking strength was linear (Bégin and Kaminska 2002). Nevertheless, these studies focused on paper that underwent hydrolytic degradation, without considering the possible effects of oxidation, and only a few instances report on the latter (Arney and Jacobs 1980; Whitmore and Bogaard 1995).

In this study, the impact of the two reactions, *i.e.*, hydrolysis and oxidation, will be considered. Because these reactions are slow under natural ageing conditions, artificial ageing of paper can be used to obtain degraded states

Published online 05 January 2024

(Bégin and Kaminska 2002; Strlič and Kolar 2005; Jeong and Potthast 2021). Although it does not exactly replicate natural ageing, this method remains valid to degrade paper since cellulose chain scissions are promoted in all cases.

The aim of the study is to determine the impact of different exposure conditions on the mechanical behaviour of paper, and more specifically on the fibre strength, the fibre-fibre bonds resistance, and the microstructure of paper. Due to the large number of structural parameters that can be involved in the embrittlement process, this multi-scale approach is applied to two papers with different microstructures. The first part focuses on the evolution of macroscopic mechanical properties of paper under artificial ageing conditions that favour either hydrolysis or oxidation reactions. Secondly, this work intends to decouple the effects on the fibres and on the fibre-fibre bonds specifically. A third part is dedicated to the evolution of the fibre resistance and the fibre-fibre bonds at the microscopic scale, allowing to relate chemical changes to macroscopic mechanical behaviour.

2 Experimental

2.1 Materials

Two different papers were used for this study. One is a commercially available paper from Canson®, grade *Barrière*, referred herein as paper A. It meets the standard for paper permanence ISO 9706. It is made from bleached kraft pulp with a mix of 50 % of long fibres (softwood) and 50 % of short fibres (hardwood), and was refined, according to the supplier. It contains about 3 % wt. of alkaline mineral particles ($CaCO_3$) to prevent the acidification. Other components, such as alkyl ketene dimer (AKD) sizing and kaolin are present in minute quantities. This paper was chosen because of its archival quality and essential durability for long-term preservation. The second paper is a filter paper Whatman n°40 made from acid-washed cotton linters (ashless grade), referred hereafter as paper B. It therefore contains only cellulose and has no additives. As opposed to paper A, it is acidic and thus prone to faster degradation. It was chosen as a model since widely studied in the paper degradation literature.

The main characteristics of papers A and B were measured, and their microstructures were observed, as summarised in **Table 1**. The methods used are defined hereafter, e.g., size and mass measurements to calculate thickness, grammage and density, MorFi analysis for fibre lengths, thermogravimetric analysis (TGA) for ash content and size-exclusion chromatography (SEC) for DP. There are major differences between the two papers, especially in terms of grammage and fibres length. In particular, paper A exhibits a significant difference between the mean length and the length-weighted length, indicating a wider length distribution than in paper B. The long fibres being responsible for the mechanical resistance, this could give paper A better strength, accordingly to the

Published online 05 January 2024

fact that it should meet the mechanical criteria of ISO 9706 standard. **Fig. 1** shows the microstructure of the surface of both papers. Paper B exhibits more fibrillation than paper A, indicating more mechanical treatment like refining during papermaking process. Paper A has also flatter fibres, in coherence with his higher density.

Table 1: Main characteristics of papers A and B. Thickness and grammage were measured using a micrometric gauge and a precision weighing scale, fibre length by MorFi analysis, ash content by thermogravimetric analysis (TGA), number-average degree of polymerisation (DP_n) of cellulose by size-exclusion chromatography (SEC), and other characteristics by microscopic observations.

Characteristics	**Paper A**	**Paper B**
Thickness (µm)	100 ± 4	210 ± 3
Grammage ($g \cdot m^{-2}$)	80 ± 4	95 ± 5
Density	0.80 ± 0.04	0.45 ± 0.02
Fibres	softwood/hardwood	cotton linters
Fibres length (µm)	508 ± 5	445 ± 5
Length-weighted fibres length (µm)	870 ± 10	750 ± 10
Ash content (%)	16.4 ± 0.6	0.4 ± 0.6
DP_n of cellulose	1870 ± 30	360 ± 10

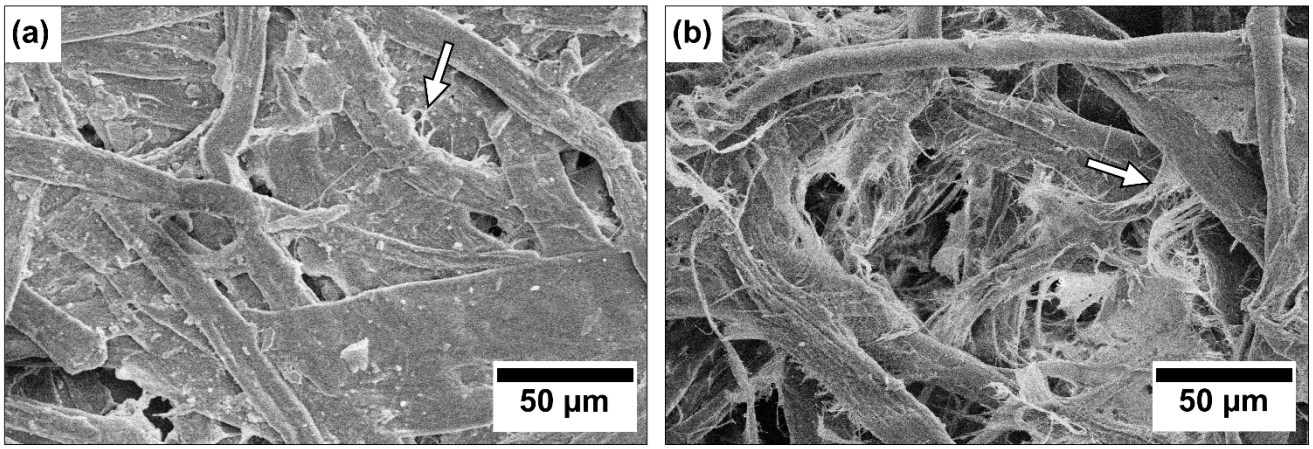

Fig. 1: Microstructure of papers A (a) and B (b) (SEM). The arrows indicate fibrillation between fibres.

2.2 Accelerated ageing

Different degradation states of the paper were achieved through exposures to artificial ageing conditions. The papers were exposed at 90 °C in closed glass tubes under different atmospheres (humid or dry, air or nitrogen) and

for different durations (e.g. 2, 4, 10, 25 and 50 weeks). Before exposure, the papers were prepared as follows: the sheets were cut in strips of 15 mm × 120 mm in the two directions of the sheet to enable mechanical testing in the main direction of the fibres (machine direction, referred hereafter as longitudinal direction) and in the perpendicular direction (cross direction, referred hereafter as transverse direction). About 20 to 30 strips (equivalent to 4 g of dry paper) were introduced in 15 cL Wheaton® glass tubes.

Two tubes per ageing duration were preconditioned under each specific atmosphere:

- 50 % RH in a climate room at 23 °C for 48 h *(humid air)*
- 0 ppm oxygen and 50 % RH in a glovebox at 23 °C for 48 h *(humid nitrogen)*
- circa 0 % RH in an oven at 105 °C for 2 h *(dry air)*
- circa 0 ppm oxygen and 0 % RH in a glovebox at 23 °C for 48 h *(dry nitrogen)*

The tubes were closed with a polypropylene screw cap and a PTFE septum insert (Duran Groups®, max. 140 °C). A three-layered film (PET, aluminium, polyethylene) was added on the tubes opening to improve tightness. They were then aged at 90 °C in the following conditions:

- 50 % RH in an environmental chamber *(humid air and humid nitrogen)*
- circa 0 % RH in an oven *(dry air and dry nitrogen)*

2.3 Chemical analysis

The degree of polymerisation (DP) of cellulose was measured by size-exclusion chromatography (isocratic HPLC pump Waters® 515 at 0.4 mL·min^{-1} and 100 µL injection volume, autosampler Dionex® UliMate 3000, 4 columns Agilent® PLGel miniMIX A (20 µm and 4.6 mm × 250 mm) thermostated at 60 °C, MALS detector Wyatt Technologies® Dawn EOS at 60 °C, differential reflective index detector Waters® 2414 at 55 °C). Samples about 10.4 mg of paper were prepared and analysed three times according to Dupont (Dupont 2003). Astra® 5.3.4.14, Wyatts Technologies® was used for the data acquisition and analysis.

The ash content in the papers was measured by thermogravimetric analysis (TGA), with a TA Instrument® TGA Q50 apparatus controlled via QSeriesTM software at a scanning speed of 10 °C per minute until 800 °C, under nitrogen at a flow rate of 90 mL·min^{-1}. The reported ash content corresponds to the relative mass remaining at 800 °C.

Published online 05 January 2024

2.4 Mechanical tests

Mechanical tests were carried out in a climate room at 23 °C and 50 % RH. The unaged and aged paper strips (15 mm × 120 mm) were conditioned for at least 48 hours in the climate room before the tests. Paper is an anisotropic material due to its fabrication process, leading to a mean orientation of the fibres along the machine direction. These tests were therefore performed in the two main directions of the sheet, *i.e.* the main direction of the fibres (machine direction), and the perpendicular axis (cross direction), referred herein as longitudinal and transverse directions, respectively.

The mechanical tests were adapted from TAPPI standards T 494 om-01 for tensile properties, T 511 om-02 for folding endurance and T 231 cm-96 for zero-span breaking strength. For tensile test, a DY20 Adamel Lhomargy dynamometer coupled with an MTS Systems® TestWorks software was used with the following setting: 5 cm of span between the jaws, speed of 1 $mm \cdot min^{-1}$, fracture detection at 50 % of the maximal stress. Folding endurance tests were realised on a Tinius Olsen® MIT folding tester at a speed of 200 folds per minute and a bending angle of 270°. The initial applied stress was equivalent to 500 g instead of 1 kg because of the low resistance of the most degraded papers. For zero-span tensile tests, a Pulmac® Z-span tester was used. The clamping pressure used was 410 kPa (60 psi), as it was the maximum stable pressure authorised by the installation and is sufficient to prevent slippage (Batchelor et al. 2006).

Each result is the average of several repeat measurements using strips from the two ageing tubes of each exposure condition. For tensile tests, 6 strips were tested for paper A, and 4 strips for paper B, in the two directions. The tests for which strips broke within 1 cm distance to the jaws were considered as invalid. For zero-span tensile and folding endurance tests, at least 10 strips were used for each paper and exposure conditions.

All the DP_n and mechanical testing data used to draw the following graphs are available in a Supplementary Information file (**Table S1**).

2.5 Observations on the microstructure

The microstructure of the paper surface was observed by scanning electron microscopy (SEM), using a Hitachi® 4800 microscope. Prior to the observation, the samples were metallised through a gold deposition process (2 minutes at 1.2 kV and 5 mA). The observations were conducted at an acceleration of 5 to 10 kV and 10 mA, and detection was performed using two secondary electron (SE) detectors positioned at high and low angles.

Published online 05 January 2024

Fracture surface of paper strips were observed through a Zeiss® SteREO Discovery V.20 binocular lens with a × 2 objective, coupled with Archimed® software. Three images were recorded for each strip at the failure zone, resulting in 18 images for each ageing condition for paper A and 12 images for paper B. These images were treated with ImageJ® software to measure the mean extracted fibre lengths at failure surface.

Microstructure characteristics of the fibres were obtained with a MorFi LB01 instrument at Pagora, Grenoble INP, France. MorFi analysis consists in gathering images of fibres in suspension. Paper is first defibrated in water; the obtained pulp is continuously pumped into the system and monitored with a speed camera. Several dozens of fibres are captured for each image, and multiple images can be recorded within a few minutes. This technique is both fast and statistical.

The samples for MorFi analysis were prepared as follows: about 2 g of paper are weighted and placed in hot water (around 65 °C) during a few hours. The volume of water is adjusted to a concentration of 1 $g \cdot L^{-1}$. The rehydrated paper is then defibred in a blunt blades pulper for 5 minutes at 50 Hz, adding 5 minutes if the defibration was not complete. Each pulp suspension is sampled in three replicas of 300 mg and ran through the MorFi machine; a fourth sample is measured in case the repeatability criteria are not met (standard deviation below 20 µm on length and 0.2 µm on diameter). MorFi software is set to stop the analysis after 50,000 elements detected as fibres (length between 0.1 and 10 mm and diameter between 5 and 75 µm) are measured.

3 Results and discussion

3.1 Macroscopic scale: mechanical behaviour

To follow macroscopic embrittlement, the behaviour of the two papers aged under different conditions and subjected to tensile test and folding endurance test is examined to evaluate the consequences of hydrolysis and oxidation reactions.

3.1.1 Embrittlement process

The stress-strain curves from tensile tests in the two main orientations of the fibres are presented in **Fig. 2** for the two papers aged under humid air conditions. The shape of the curves is characteristic of the elastoplastic behaviour of paper (Hill et al. 1995; Fernández-Diego et al. 2021). First, the mechanical properties at the unaged stage are presented in order to exhibit the structure-properties relationship for the two papers **(Table 2)**. Stress at break and elastic modulus are normalised by the density of the papers. Brittleness index is defined by Zou as the ratio of elastic strain energy to the total tensile energy absorption (TEA) at the time of failure (Zou et al. 1994).

Published online 05 January 2024

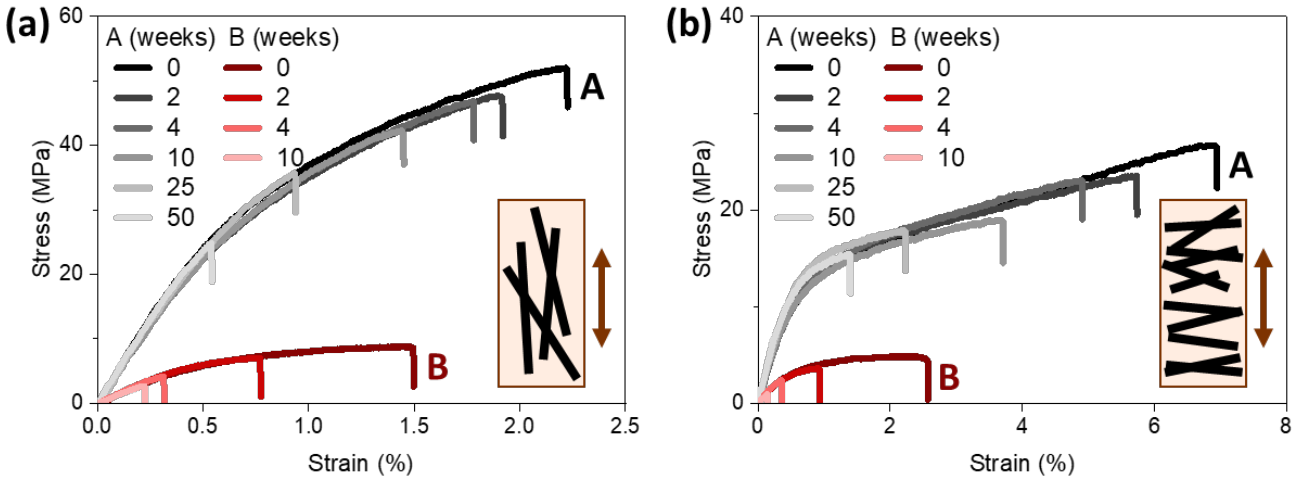

Fig. 2: Stress-strain curves for papers A and B in the longitudinal direction of the fibres (a) and in the transverse direction (b), at unaged state and after ageing for 2 to 50 weeks under humid air conditions.

Table 2: Tensile properties of unaged papers A and B in longitudinal and transverse directions: stress at break and elastic modulus are normalised, *i.e.* divided by the density of paper. Brittleness index is the ratio of elastic strain energy to the total tensile energy absorption at the time of failure.

	Paper A		**Paper B**	
	Longitudinal direction	Transverse direction	Longitudinal direction	Transverse direction
Normalised stress at break (MPa)	58.5 ± 1.9	29.9 ± 1.6	19.4 ± 0.3	10.4 ± 0.7
Strain at break (%)	2.2 ± 0.2	6.4 ± 0.7	1.5 ± 0.1	2.3 ± 0.2
Normalised elastic modulus (GPa)	5.9 ± 0.2	2.9 ± 0.3	3.0 ± 0.1	1.8 ± 0.1
Brittleness index (%)	33.8 ± 3.4	10.7 ± 0.8	42.1 ± 3.6	25.6 ± 4.4

Large discrepancies between paper A and paper B were found **(Table 2)**: at unaged state, paper B has smaller normalised stress at break, normalised elastic modulus, and strain at break than paper A in both directions. Its brittleness index is higher, corresponding to a more fragile behaviour. To explain these observations, the initial characteristics of the papers were measured (**Table 1)**. Even if paper B exhibits higher degree of refining (**Fig. 1**), it has a lower density, slightly shorter fibres, and a considerably lower DP_n of cellulose, all of which suggests weaker network and weaker fibre resistance (Bronkhorst 2003; Picu 2021). Moreover, the papermaking process

of paper A includes the addition of strengthening agents such as the sizing. Its higher strength is coherent with its use as a printing paper, compared to paper B, which is designed for filtering and hence has no additives. Paper A is also more rigid than paper B as indicated by the much higher elastic modulus. This can be explained by its higher density that increases the probability of fibre-fibre bonding, which is responsible for more rigid networks.

Table 2 also shows the anisotropy of the papers: as expected, the transverse direction exhibited smaller normalised elastic modulus and brittleness index, leading to larger strain at break for both papers (Cox 1952; Leheny et al. 2021). The anisotropy can be quantified through the ratio of elastic modulus in longitudinal to transverse direction. This ratio is 2.0 in the case of paper A, and 1.7 for paper B. The larger anisotropy of paper A can be explained by a different fabrication process. Moreover, in the inelastic zone of the strain-stress curve, the slope is smaller in the transverse direction. The difference in the inelastic behaviour is also linked to the fibre orientation. This could be explained by rearrangement processes: in the transverse direction, the fibres have more degree of freedom to align with the tensile axis than in longitudinal direction. This leads to two to three times higher strain at break.

As shown on **Fig. 2**, the artificial ageing leads to earlier failure: the strength and the strain at break decrease, but the elastic modulus remains stable, as confirmed by the literature (Kurei et al. 2022). The embrittlement of paper B occurs for shorter exposure times than that of paper A. After a 10-week ageing, it reaches a strength for which paper is hardly manipulable. The evolution of the mechanical properties with ageing is presented below.

3.1.2 Correlation between mechanical properties and chemical degradation

The detailed evolution of tensile test parameters is illustrated in **Fig. 3** for both papers aged under the different exposure conditions, and in the two main directions. The chemical degradation state is expressed in terms of number-average degree of polymerisation (DP_n), value used to calculate the length of cellulose chain, knowing that both ageing mechanisms, hydrolysis and oxidation, lead to chain scissions. DP_n data for paper A and B aged under humid air, humid nitrogen, and dry air up to 10 weeks have been presented from a kinetic point of view in recent work (Vibert et al. 2023). It showed in particular that the presence of oxygen enhanced the degradation of both papers, and that the degradation of paper B was faster than that of paper A whatever the ageing condition.

Published online 05 January 2024

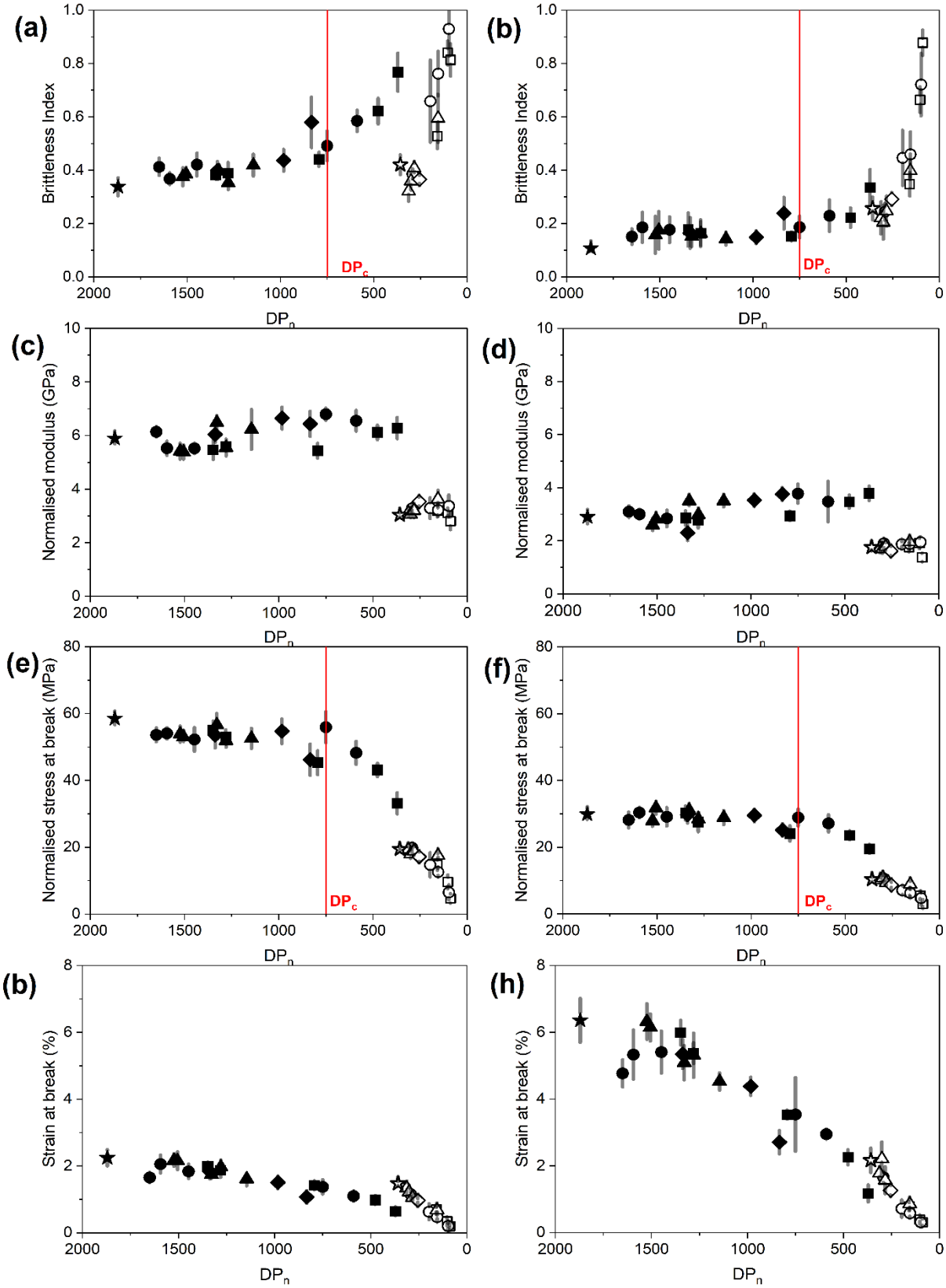

275

276 **Fig. 3**: Evolution of mechanical properties with the decrease of degree of polymerisation, as measured by tensile
277 test for the two papers in the longitudinal direction (a, c, e, f) and in the transverse direction (b, d, f, h) upon all
278 exposure conditions for different durations between 0 and 50 weeks at 90 °C (initial values ★, humid air ■,

279 humid nitrogen ●, dry air ▲, dry nitrogen ◆, full symbols for paper A and empty symbols for paper B). The
280 vertical red line indicates the value of critical DP_n.

281 **Fig. 3** shows that the evolution of the mechanical parameters of the two papers followed the same trend
282 independently of the orientation of the fibres and the exposure conditions. Papers become increasingly more brittle
283 as shown by the increase of the brittleness index, and a concomitant decrease of the stress and the strain at break,
284 while the elastic modulus remains constant.

285 Interestingly, the data points for a given paper and direction align on a unique curve as a function of DP_n. In other
286 words, the embrittlement process is independent of the exposure conditions. This confirms the zero-span tensile
287 strength data of Zou for acidic paper (Zou et al. 1994). However, to our knowledge in the case of permanent paper,
288 which is reported to be more prone to oxidation (Kolar 1997), this result had not been reported before. In particular,
289 it demonstrates that, even when oxidation plays a role in the chemical degradation (Vibert *et al.*, 2023), this does
290 not lead to a different mechanical behaviour of the paper. The influence of oxidation on the embrittlement process
291 could have been expected as certain types of oxidation mechanisms could impact hydrogen bonding, as for
292 example the oxidation of hydroxyl groups into carbonyl groups along the glucose ring (Kolar 1997). However,
293 this has been shown to be negligible (Ahn et al. 2012). This would have reduced the number of donors of hydrogen-
294 bonds, which are responsible for bonding in the fibres, and at fibre-fibre bonds. In this study, such behaviour was
295 not observed, thus oxidative exposure conditions do not lead to fibre-fibre bonds degradation.

296 **Fig. 3** also exhibits the existence of a critical DP for paper A, under which the decrease of normalised stress at
297 break accelerates. According to the brittleness index and to the normalized stress at break as a function of DP_n, the
298 critical DP_n associated to the beginning of the embrittlement process lies between 500 and 1000. The existence of
299 a critical *DP* (DP_c) was notably shown in the literature in relation with the zero-span tensile tests (Zou et al. 1993);
300 this point will be discussed below. It was not observed for paper B, for which the initial DP_n value is already below
301 500 due to the acidic manufacturing process, which decreases the DP.

302 A slight decrease in the slopes of the curves on **Fig. 3** prior to reaching the DP_c, after which a more significant
303 decrease of the mechanical property occurs, was observed for both stress at break and brittleness index of paper
304 A. Conversely, the strain at break exhibited an almost linear decrease, and again no evolution was observed for
305 the elastic modulus. This latter observation is consistent with the literature (Zou et al. 1994; Kurei et al. 2022).
306 Since the elastic modulus is partly related to the elasticity of fibre-fibre bonds, the authors suggested that its
307 constancy may be explained by the absence of degradation of the bonds.

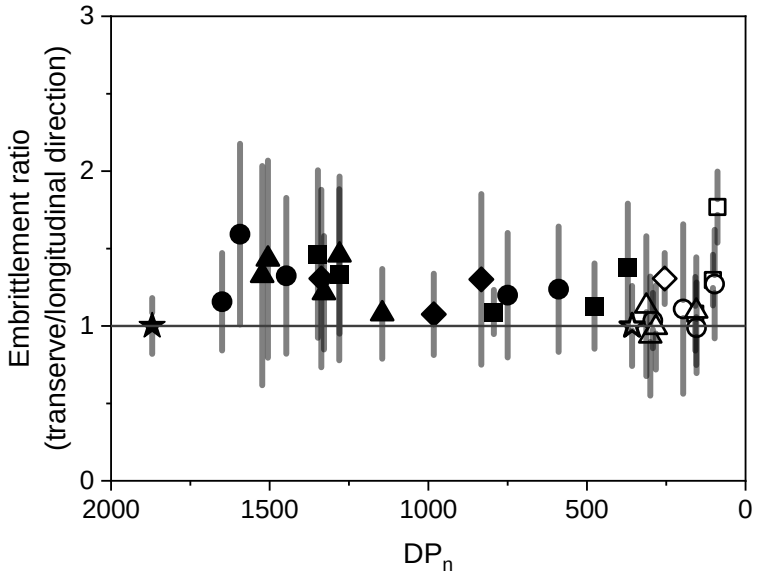

Fig. 4: Embrittlement ratio (transverse *vs* longitudinal directions variation in the brittleness index) as a function of DP_n (initial values ★, humid air ■, humid nitrogen ●, dry air ▲, dry nitrogen ◆, full symbols for paper A and empty symbols for paper B).

To illustrate the relative variation of the mechanical properties as a function of the direction of the stress, and hence the influence of the orientation of the fibres in the embrittlement process, an embrittlement ratio is shown in **Fig. 4**. This embrittlement ratio (ER) was calculated as the embrittlement in the transverse direction (T) over the embrittlement in the longitudinal direction (L) of the fibres, the embrittlement being the variation of brittleness index with ageing, *i.e.* the brittleness index at a given degraded state BI(t) over the initial state BI(0):

$$ER(t) = (BI_T(t) / BI_T(0)) / (BI_L(t) / BI_L(0)) \quad (1)$$

ER expresses if one direction exhibits faster embrittlement than the other. This ratio remained above 1 for both papers, showing that the transverse direction underwent faster embrittlement than the longitudinal direction $(BI_T(t) / BI_T(0)) > (BI_L(t) / BI_L(0))$. In the longitudinal direction, the fibres are aligned with the direction of the principal stress, and the fibre-fibre bonds are under little stress. On the contrary, in the transverse direction, the fibres are oriented perpendicular to the load direction, which leads to the fibre-fibre bonds being sheared. Moreover, in the latter configuration, the reorientation of the fibres during the mechanical loading also leads to bending the fibres (Deshpande et al. 2001; Syerko et al. 2012). It can be concluded that during ageing, either the fibre-fibre bonds are damaged, or the fibres are less resistant to bending. Since the constancy of elastic modulus gave clues for bonds stability, the second hypothesis applies.

Published online 05 January 2024

3.1.3 Fatigue properties: folding endurance

The papers were also tested for mechanical fatigue in the longitudinal direction. Folding endurance is a localised bending fatigue test. The results for all the ageing conditions are shown in **Fig. 5**. Again, the decrease in the folding endurance does not depend on the ageing condition. It appears to be linear with the DP_n for paper B, as well as for paper A up to approaching degradation levels corresponding to the DP_c. This critical DP_n, identified by the slope break, is again around 750. The slope is also stiffer than for tensile properties as a function of DP_n, similarly to tensile fatigue tests that highlight the effect of chemical degradation (Yue et al. 2019).

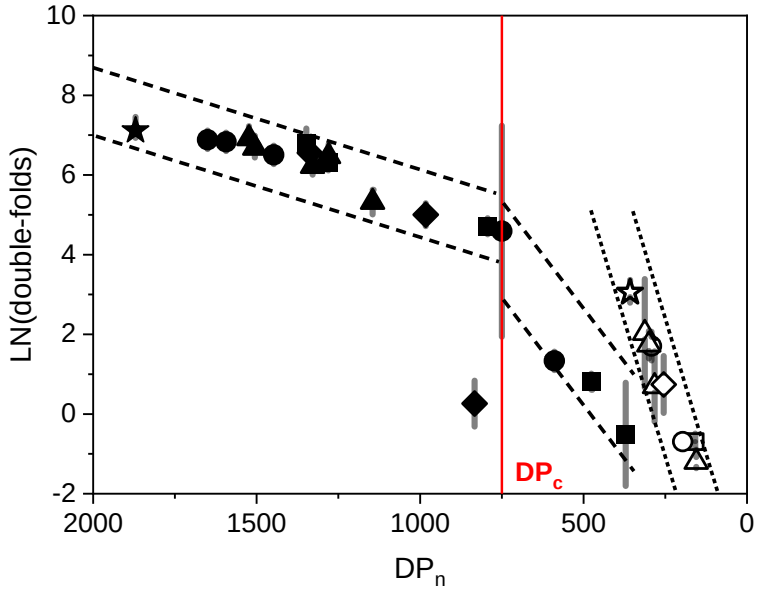

Fig. 5: Evolution of the folding resistance in longitudinal direction with the degradation, as expressed as the logarithm of the mean number of double-folds at break (initial values ★, humid air ■, humid nitrogen ●, dry air ▲, dry nitrogen ◆, full symbols for paper A and empty symbols for paper B). The vertical red line indicates the value of critical DP_n.

It is interesting to note that the critical DP_n for folding endurance to start showing a faster decay is the same as for stress at break. This suggests that the damage mechanisms in the folding and tensile tests are bound to similar chemical degradation mechanisms. For both tests, stress is applied on both fibres and fibre-fibre bonds. However, during folding, bending applies more on the fibres than on the bonds because the strain is localised on a precise section of the paper. During tensile tests, the stress is distributed in all the sample, and applies to both fibres and fibre-fibre bonds. Therefore, the stress applied on the fibre-fibre bonds is different for tensile and folding test. This would suggest that the DP_c mechanism relates more specifically to the fibre and not to the fibre-fibre bonds.

Published online 05 January 2024

3.2 Mesoscopic scale: decoupling the mechanical behaviour of fibre and fibre-fibre bonds

The decrease in paper strength relates to the location of the embrittlement mechanism, predominantly at fibre-fibre bonds or within the fibres. To decouple the effects, the zero-span tensile test was used as a fibre-specific test, providing information on the intrinsic degradation of the fibres.

3.2.1 Zero-span tensile tests

Fig. 6 shows the normalised zero-span tensile strength of the two papers aged in the different conditions. Confirming the earlier results on the tensile properties, for a given paper and in a specific direction all the data points aligned on the same curve, showing no individual effect of the oxidation or the hydrolysis on the mechanical degradation of fibres. As with the other mechanical tests, differences between the papers and dependency on the fibre's direction are visible.

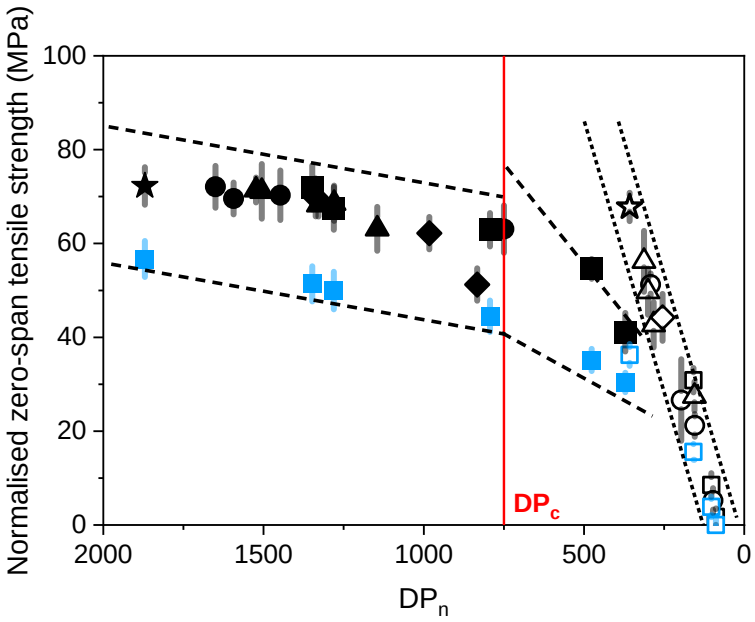

Fig. 6: Zero-span tensile strength normalised by the density of paper in the two principal directions *vs* DP_n (initial values ★, humid air ■, humid nitrogen ●, dry air ▲, dry nitrogen ◆, full symbols for paper A and empty symbols for paper B, black for longitudinal direction and light blue for transverse direction). The vertical red line indicates the value of critical DP_n.

The value of zero-span tensile strength of the unaged samples in the transverse direction is higher than that for the stress at break in the normal tensile test, being 72.3 and 58.5 MPa for paper A and 67.8 and 19.4 MPa for paper B, respectively. This can be due to the fact that zero-span tensile test is localised (Wathén et al. 2005), *i.e*. the stress

is applied on both sides of a section of the sheet. The resulting strength is the average strength of a randomly selected section in the paper sheet, whereas during tensile test, the paper sheet breaks at the weakest section.

As for tensile test, in the transverse direction, the zero-span resistance is lower than in the longitudinal direction at all equivalent degradation states and conditions. By volume conservation, the surface of fibres in a longitudinal as in a transverse section is the same. However, due to the alignment of cellulose chains in the crystallites almost parallelly with the direction of the fibre (Young and Rowell 1986), fibres should be more resistant under longitudinal tensile, where cellulose chains are stressed, than under transverse tensile, where hydrogen bonds between cellulose chains are. The higher zero-span tensile strength in the longitudinal direction of the paper can simply be explained by the much larger number of fibres passing through a given section if the latter is perpendicular to the direction of fibres than if it is parallel to the direction of fibres.

As observed for other tests, paper A exhibited a shallow decrease in the high DP_n ranges, and a steeper decrease after the DP_c = 750. This would indicate that the embrittlement mechanism is more related to the fibre than to the fibre-fibre bond. Again, no slope break, and hence no critical DP_n, was observed for paper B for which the initial DP_n is already below 750. This is consistent with the literature, where a critical *DP* in zero-span tensile test was observed between 500 and 1000 (Zou et al. 1994; Tétreault et al. 2019). However, to our knowledge, no explanation for the existence of a critical value has been proposed. Such degree of polymerisation threshold has been observed for conventional semi-crystalline polymers (Fayolle et al. 2008). It is associated with the critical molar mass to ensure a minimum thickness of amorphous phase, which is responsible for plastic deformation mechanisms. However, the specific fibrillar and microfibrillar structure of cellulose adds a level of complexity. Given the fibre morphology, schematised in **Fig. 7**, a *DP* of 750 corresponds to 4 or 5 units of crystalline plus amorphous zones, considering that the crystallinity of paper is 70 % and that the LODP of 100 corresponds to the average length of a crystallite (Young and Rowell 1986). It also corresponds to an average of 1.5 scissions per cellulose chain for paper A. This might be the average degradation level under which transfer of applied stress along the fibres and through fibre-fibre bonds becomes less efficient.

Published online 05 January 2024

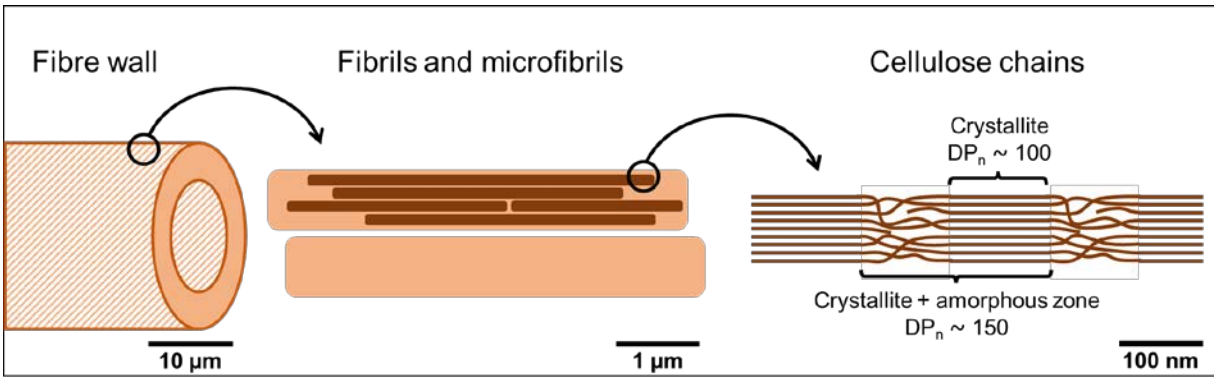

Fig. 7. Schematic representation of the microstructure of a cellulose fibre at the scale of the fibre, the fibrils, and the cellulose chains according to (Kortschot 1997) and (Young and Rowell 1986).

3.2.2 Page equation

The results of the zero-span tensile tests and of the tensile strength tests showed the evolution of the paper strength. The comparison between these values can be used to assess the contribution of fibre-fibre bonds to the paper strength, and how it evolves with ageing. In this regard, the semi-empirical Page equation relates the two tests as follows (Page 1969):

$$1/L_T = 9/8 * 1/L_Z + 12g/bL\alpha \quad (2)$$

with L_T and L_Z being respectively the breaking length in tensile and in zero-span tensile test (in km), *i.e.*, the equivalent length of paper for which the strip breaks under its own weight, g the standard acceleration due to gravity, b the surface shear bonding strength (in $kg \cdot m \cdot s^{-2}$), L the mean fibre length (in m), and α the contact area relative to the mass of paper (in $m^2 \cdot g^{-1}$). $bL\alpha$ represents the shearing bonding of the paper. This equation expresses the fact that tensile resistance arises both from fibre resistance and fibre-fibre bonding.

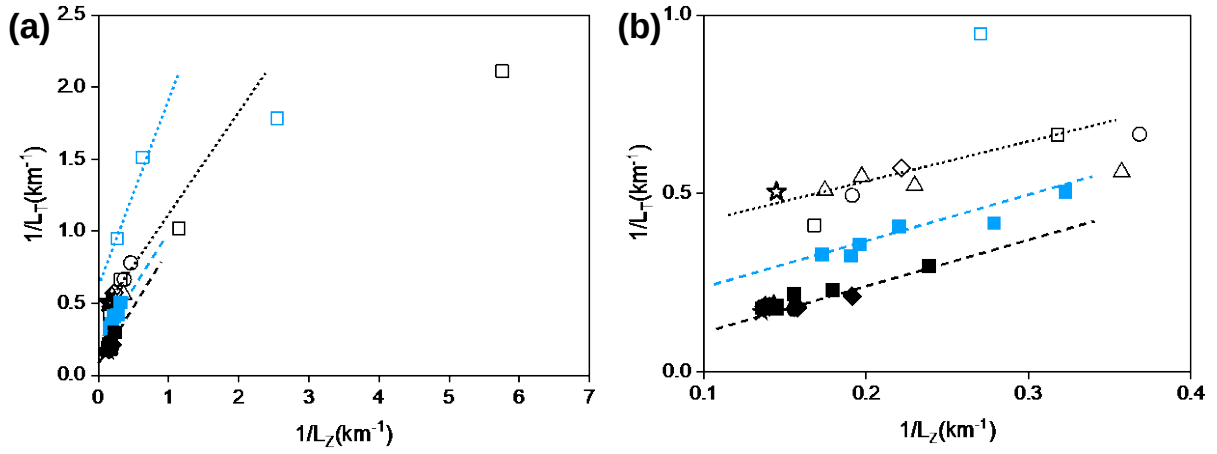

Fig. 8: (a) Graphical representation of the Page equation for papers A and B, with L_T the tensile breaking length and L_Z the zero-span breaking length. The data points in the lower inverse length area being aggregated, (b) zoom of (a) (initial values ★, humid air ■, humid nitrogen ●, dry air ▲, dry nitrogen ◆, full symbols for paper A and empty symbols for paper B, black for longitudinal direction and light blue for transverse direction).

Table 3: Parameters of the Page equation for papers A and B: $1/L_T = a\ /L_Z + 12g/bL\alpha$, with the correlation coefficient r^2 for papers aged under humid air.

Paper	**Direction**	**Exposure condition**	***a***	**r^2**	***bLα* ($km^2 \cdot s^{-2}$)**
A	Longitudinal	humid air	1.18	0.97	6.8
		all conditions	1.08	0.85	4.3
	Transverse	humid air	1.11	0.91	0.9
B	Longitudinal	humid air *	1.20	0.77	0.4
		all conditions *	0.80	0.78	0.3
	Transverse	humid air *	1.57	/	0.2

* For paper B, the data for 4 and 10 weeks under humid air conditions were not included because of excessive damage.

To assess the validity of Page model in the case of artificial ageing of paper due to hydrolysis and oxidation, tensile and zero-span breaking lengths were plotted in **Fig. 8**. The curve was not linear for high values of $1/L_T$. However, most data set points of a same paper and orientation were aligned. The four data points that exhibited non-linear behaviour correspond to the highest degradation states of paper B, *i.e.* aged for 4 and 10 weeks in humid air conditions. In terms of *DP*, these samples have reached the levelling-off degree of polymerisation (LODP), e.g. the *DP* for which where the kinetics of cellulose hydrolysis slows down tremendously (Battista et al. 1956; Stephens et al. 2008). At this advanced stage of degradation, Page model is no longer valid. However, it is interesting to note that Page equation is valid before reaching the LODP, even for DP values lower than the DP_c of 750 defined previously.

The parameters in the Page equation were assessed in the linear regime of the slopes. **Table 3** presents the results of the linear regressions. The slope, named *a*, between zero-span and tensile breaking lengths is found to be close to 9/8 for both papers. In Page's equation, this value of 9/8 accounts for the Poisson ratio of the paper being of 1/3. As a comparison, Zou found a slope around 1.25 for the same paper as paper B aged in humid air, which is slightly above that of Page (Zou et al. 1994). It is not surprising that the slopes that were found here are not exactly those

of Page or Zou, according to the fact that the Poisson ratio of the paper depends on the fibre orientation (Cox 1952), and may depend on the nature and processing of the fibres.

Furthermore, **Table 3** shows that the linear regression is less accurate when all the data points are included. Since the ageing conditions were found to have no differentiated impact on the mechanical embrittlement, this observation can be explained by the fact that, except for the humid air condition, the embrittlement level is low, and the data points are therefore clustered.

Page equation also gives an estimate of the shear bonding $bL\alpha$. This parameter is reported in **Table 3.** It is higher for paper A than for paper B. This can be explained by a difference in bonding strength, in fibre length, or in contact area. As shown in **Table 1**, the fibres in paper A are in average longer by 15 % than in paper B and the density of paper A about two times higher. Assuming that density is almost linear with contact area (Sampson 2003) , the α parameter of paper A is also twice that of paper B. Taking into account these ratios, the surface shear bond b in paper A would be around 8 times higher than that in paper B.

Table 3 shows an unexpected difference between the longitudinal and transverse directions, even more pronounced for paper A. Indeed, according to the definition provided by Page, none of the b, L and α parameters are defined as dependent on the direction of the fibres. However, it can be presumed that b is in fact dependent on the orientation, as it can account for the projection of bonding shear along the considered axis. This explanation is consistent with the fact that fibre-fibre bonds are not submitted to the same stress depending on the orientation.

3.3 Microscopic scale: Morphology of the fibres

The microstructure of paper was evaluated using two different and complementary techniques: localised observations of the fracture surfaces to obtain *in situ* information, and MorFi analysis that enables a statistical evaluation of the morphology of fibres.

3.3.1 Fracture surfaces

To evaluate the impact of ageing on the rupture mechanism of the papers, the fracture surfaces after tensile tests were observed and the length of pulled-out fibres was measured. The results, reported in **Fig. 9**, show that the pull-out length decreased for both papers as function of DP_n. Furthermore, this evolution seems almost linear with DP, with a steeper slope for paper B than for paper A.

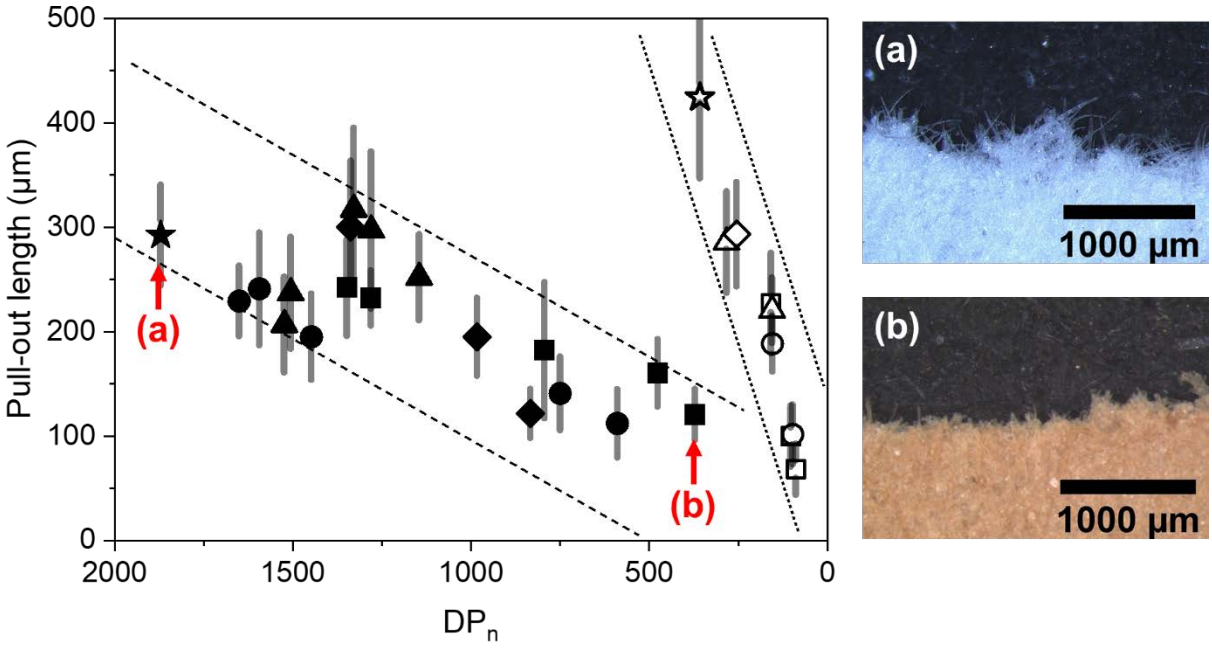

450

451 **Fig. 9**: Evolution of the mean length of the pulled-out fibres in the fracture zone for longitudinal direction tensile
452 tests (Δ = 50 µm) as a function of DP_n (initial values ★, humid air ■, humid nitrogen ●, dry air ▲, dry nitrogen
453 ◆, full symbols for paper A, and empty symbols for paper B). Microscopy images of fracture surfaces for paper
454 A at initial state (a) and after 50-week in humid air (b).

455 The pull-out length depends on the slippage of fibres at the fracture surface (Wathén et al. 2005). If the fracture is
456 due to the rupture of the fibre-fibre bonds (**Fig. 10a**), the fibre at fracture surface would entirely slip out the
457 network, and the pull-out length would be in average equal to half the fibre length (as half of the fibre would stay
458 in each part of the broken strip, in average). On the contrary, if the fracture is due to rupture of the fibres while the
459 fibre-fibre bonds remain constant (**Fig. 10b**), only the length equivalent between two bonds would slip, and the
460 pull-out length would be equal to half of the average bond-to-bond length.

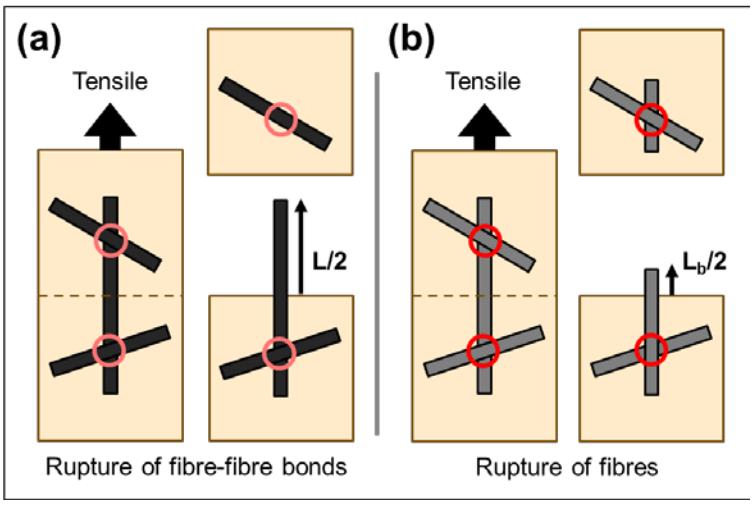

461

Fig. 10: Scheme of the pull-out length at fracture surface for embrittlement of either fibre-fibre bonds (red circles) (a) or fibres (b), with L the fibre length and L_b the bond-to-bond length.

The initial pull-out length of paper A and B are about 300 µm and 550 µm, respectively. Compared to the fibre length of both papers (508 and 445 µm, respectively (**Table 1**)), these values are significantly higher than expected, *i.e.* 254 and 223 µm maximum, respectively. This can be explained by a measurement bias. Indeed, the longer pulled-out fibres are better detected in the binocular lens images, and the smaller fibres might not be measured using ImageJ® software. The measured pull-out length is therefore higher than the actual pull-out length. However, since measurements and image treatments were done in the same manner for all the images, the comparison upon ageing is still relevant.

It can also be stressed out that, at the initial stage, paper B exhibited longer extracted fibres than paper A, even if its fibres are in average shorter. This can be justified by the differences in the average number of contacts and fibre-fibre bonding strength. The lower density of paper B could explain less contact between the fibres, and therefore longer bond-to-bond length. On the other hand, the absence of additives, such as AKD sizing or fillers, induces weaker bonding between fibres. These two factors lead to longer pull-out. Moreover, the presence of fine elements and strengthening additives can reinforce the bounding, and thus a lower pulled-out length. This can also explain the stiffer slope (**Fig. 9**), as fibre strength becomes all the more predominant in pull-out lengths in the case of paper B.

The general decrease of pull-out length can be interpreted as a decrease of the fibre strength. Indeed, if the fibre strength remained constant, the fibre-fibre bonds should be responsible for the diminution. To achieve such diminution, it would require a decrease of bond-to-bond length, *i.e.* an increase of the number of fibre-fibre bonds, or an increase of bonding strength. None of these hypotheses have been reported in the literature, nor do they seem consistent with chemical degradation or paper morphology. Fracture surfaces provide therefore further evidence of the embrittlement being due a decrease in the fibre strength.

3.3.2 Fibres length and shape

The morphology features of fibres were measured using a MorFi analyser. This technique is based on image analysis of paper pulp, e.g., fibres in suspension in water. It has to be noted that the repulping process induces mechanical stress on the fibres during their separation, which can lead to earlier fibre break. The length measured by MorFi is therefore referred hereafter as repulped fibre length, as opposed to *in situ* fibre length. Moreover, the

image analysis can induce a bias since only elements with sizes included between 0.1 and 10 mm length and between 5 and 75 µm thick are considered as fibres by the software, smaller elements being considered as fines.

Table 4: Morphological parameters of the fibres and pulps as measured with MorFi: arithmetical mean length of fibres (standard deviation: Δ = 5 µm), length of fine elements over the total length of detected objects (Δ = 2 %), percentage of kinked fibres (Δ = 0.4 %), for unaged paper and paper aged under humid air conditions.

Paper	Ageing (weeks)	DP_n	Length (µm)	Fine elements (%)	Kinked fibres (%)
Paper A	0	1870	508	37	14.8
	2	1348	504	41	15.0
	4	1281	497	41	14.5
	10	793	494	42	15.0
	25	476	480	41	14.2
	50	371	475	39	14.2
Paper B	0	358	445	29	16.1
	1	326	451	27	16.3
	2	159	455	25	17.0
	4	103	306	48	6.1
	10	88	276	61	3.8

The evolution of the repulped fibre length upon ageing is presented **Table 4**. The ageing leads to a decrease of the fibre length in both papers. It is interesting to note that this diminution is significant for paper B after 4 weeks of ageing, considering the standard deviation of 5 µm, with the length decreasing by 38 % for 75 % decrease of DP_n, compared to 6 % for paper A for 80 % decrease of DP_n. This degradation state corresponds to the reach of LODP, i.e., the chemical degradation state for which cellulose becomes less accessible, as observed in the case of the graphical representation of Page equation where a plateau is reached (section 3.2.2). A faster weakening of the fibres after LODP can explain the abrupt decrease of repulped fibre length between 2 and 4 weeks of ageing. The non-linearity observed after LODP implies that $bL\alpha$ parameter of Page equation can no longer be considered constant. It is also noteworthy that no specific behaviour related to the repulped fibre length can be observed at the DP_c of 750.

The abrupt change in average length in the case of paper B was related to other morphological parameters. **Table 4** shows that this phenomenon is accompanied by an increase in the proportion of fine elements, and a drastic reduction of the percentage of kinked fibres. This evidences the fact that fibres break more easily, and the smaller parts of broken fibres no longer account as fibres but as fines. Moreover, the rupture of fibres most probably occurs at fibre kinks, explaining why the number of kinked fibres decrease. The production of fines from fibre breaks would only happen for a fraction of the broken fibres, justifying why the increase of the proportion of fines is lower that the decrease of kinked fibres. This seems to happen for DP_n lower than 100, and was thus not observed in the case of paper A.

Two phenomena can be put forward to explain specific breakage at kinks. On the one hand, if a kinked fibre is stressed at its extremities, the kink will be bent due to a localised concentration of stress (Aslan et al. 2011; Richely et al. 2022). This would lead to breaking at kinks. A homogenous chemical degradation along the fibre could thereupon lower the breaking criteria of kinks, allowing increasingly more fibre rupture during MorFi sample preparation, and thus a decrease of repulping fibre length. On the other hand, kinks are defects created in the fibres during the papermaking process. It can induce failures in both amorphous and crystalline zones (Ciesielski et al. 2019), leading to less ordered cellulose. Chemically reactive sites could be more accessible to reactants, and thus more prone to degradation. More degradation in these areas would lead to less resistance of the fibres. This would mean that cellulose chains break at specific locations, leading to low and heterogenous chemical degradation. Even though possible, this was not observed for the papers tested (Vibert et al. 2023). Breakage at kinks is thus principally due to stress concentration, and the second phenomenon might happen to a lesser extent.

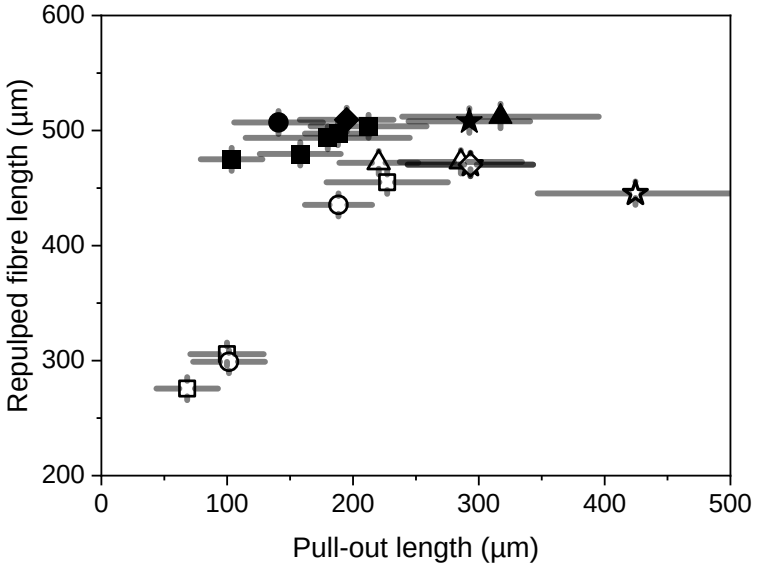

Fig. 11: Length of fibres measured in MorFi compared to the length of pulled-out fibres measured by microscopy at fracture surface (initial values ★, humid air ■, humid nitrogen ●, dry air ▲, dry nitrogen ◆, full symbols for paper A and empty symbols for paper B).

The fibre length obtained with MorFi analysis was compared to the length of the fibres at the fracture surface. The results are presented on **Fig. 11**. For paper A, it shows that extracted lengths decrease more rapidly than repulped fibre lengths. For paper B, the slope is constant only at low degradation levels after which it shows a linear correlation for samples with *DP* below 250.

As already mentioned (section 3.3.1), the relationship between extracted length and fibre length could give insight in the breaking mechanisms. On **Fig. 11**, the slope for paper A is 0.1, while the slope for paper B is close to zero for low degradation levels and is 1.4 for higher degraded states. If we assume that the extraction length depends on the fibre length, the correlation would be linear with a slope of 2. Indeed, for fibres that in average break in the middle, when the fibre shortens by 1, the extracted length shortens by 0.5. Therefore, it can be concluded that the evolution of the extracted length is not due to fibre shortening, but to a diminution of the fibre strength.

4 Conclusions

In conclusion, the results indicated that the embrittlement mechanism of paper was not affected by the exposure conditions, since oxidative and hydrolytic exposure conditions lead to similar effects. The embrittlement process is essentially driven by the reduction of degree of polymerisation by cellulose chain scissions.

The evolution of paper mechanical behaviour with ageing is primarily attributed to the embrittlement of the fibres rather than to the fibre-fibre bonds modifications, as evidenced by the validity of Page equation. Testing the paper in the transverse direction of the fibres allowed for the characterisation of the network by varying the ratio of fibres to fibre-fibre bonds, which helped to confirm the first hypothesis.

A critical degree of polymerisation was identified around DP_n of 750 in the case of paper A, below which the embrittlement occurs more significantly. The existence of this critical *DP* was confirmed by zero-span tensile tests, indicating that the damage mechanism is localised in the fibre.

The fracture preferentially occurs at morphological defects along the fibres, as highlighted by MorFi measurements for different states of paper degradation. This is not necessarily a symptom of heterogeneous degradation, but more likely a concentration of stress at the kinks leading to early breakage in the conditions of the MorFi analysis.

Published online 05 January 2024

5 Statements & Declarations

Ethics approval and consent to participate

Not applicable.

Consent for publication

All the authors give their consent for the publication of this manuscript.

Availability of data and materials

Data will be available upon reasonable request.

Competing interests

The authors have no relevant financial or non-financial interests to disclose.

Funding

Not applicable.

Authors' contribution

Caroline Vibert: Conceptualization, Methodology, Investigation, Writing - Original Draft, Visualization; Anne-Laurence Dupont: Resources, Writing - Review & Editing, Supervision, Project administration, Funding acquisition; Justin Dirrenberger: Supervision, Funding acquisition; Raphael Passas: Resources, Data Curation, Writing - Review & Editing; Denise Ricard: Resources, Funding acquisition; Bruno Fayolle: Writing - Review & Editing, Supervision, Project administration, Funding acquisition.

Acknowledgements

The work was financially supported by the French National Agency for Radioactive Waste Management (Andra). Hugo Mouchard is warmly thanked for his technical contribution. The financial support of the French Conservatory of Arts and Crafts (CNAM) is gratefully acknowledged.

6 References

Ahn K, Hennniges U, Banik G, Potthast A (2012) Is cellulose degradation due to β-elimination processes a threat in mass deacidification of library books? Cellulose 19:1149–1159. https://doi.org/10.1007/s10570-012-9723-3

Ali I (2012) Study of the mechanical behavior of recycled fibers. Applications to papers and paperboards. Université de Grenoble

Arney JS, Jacobs AJ (1980) The influence of temperature on the relative contribution of oxygen-independent and oxygen-dependent processes in the total rate. TAPPI Journal 63:75–77

Aslan M, Chinga-Carrasco G, Sørensen BF, Madsen B (2011) Strength variability of single flax fibres. J Mater Sci 46:6344–6354. https://doi.org/10.1007/s10853-011-5581-x

Bache-Wiig J, Henden PC (2010) Measurements on microtomographic images of fibrous structures: Individual fiber segmentation of 3D microtomograms of paper and wood fiber- reinforced composite materials, LAP Lambert Academic Publishing. London, United Kingdom

Barbier C, Dendievel R, Rodney D (2009) Role of friction in the mechanics of nonbonded fibrous materials. Phys Rev E 80:1–5. https://doi.org/10.1103/PhysRevE.80.016115

Barrow WJ, Sproull RC (1959) Permanence in Book Papers. Science 129:1075–1084

Batchelor WJ, Westerlind BS, Hägglund R, Gradin P (2006) Effect of test conditions on measured loads and displacements in zero-span testing. Tappi Journal 5:3–8

Battista OA, Coppick S, Howsmon JA, et al (1956) Level-Off Degree of Polymerization. Ind Eng Chem 48:333–335. https://doi.org/10.1021/ie50554a046

Bégin PL, Kaminska E (2002) Thermal Accelerated Ageing Test Method Development. Restaurator 23:89–105. https://doi.org/10.1515/REST.2002.89

Bronkhorst CA (2003) Modelling paper as a two-dimensional elastic–plastic stochastic network. International Journal of Solids and Structures 40:5441–5454. https://doi.org/10.1016/S0020-7683(03)00281-6

Carrascal IA, Fernández-Diego C, Casado JA, et al (2018) Quantification of Kraft paper ageing in mineral oil impregnated insulation systems through mechanical characterization. Cellulose 25:3583–3594. https://doi.org/10.1007/s10570-018-1788-1

Ciesielski PN, Wagner R, Bharadwaj VS, et al (2019) Nanomechanics of cellulose deformation reveal molecular defects that facilitate natural deconstruction. PNAS 116:9825–9830. https://doi.org/doi.org/10.1073/pnas.1900161116

Cox HL (1952) The elasticity and strength of paper and other fibrous materials. Br J Appl Phys 3:72–79. https://doi.org/10.1088/0508-3443/3/3/302

Deogekar S, Islam MR, Picu RC (2019) Parameters controlling the strength of stochastic fibrous materials. International Journal of Solids and Structures 168:194–202. https://doi.org/10.1016/j.ijsolstr.2019.03.033

Deshpande VS, Ashby MF, Fleck NA (2001) Foam topology: bending versus stretching dominated architectures. Acta Materialia 49:1035–1040. https://doi.org/10.1016/S1359-6454(00)00379-7

Driemeier C, Mendes FM, Oliveira MM (2012) Dynamic vapor sorption and thermoporometry to probe water in celluloses. Cellulose 19:1051–1063. https://doi.org/10.1007/s10570-012-9727-z

Dupont A-L (2003) Cellulose in lithium chloride/N,N-dimethylacetamide, optimisation of a dissolution method using paper substrates and stability of the solutions. Polymer 44:4117–4126. https://doi.org/10.1016/S0032-3861(03)00398-7

Emerson MJ, Jespersen KM, Dahl AB, et al (2017) Individual fibre segmentation from 3D X-ray computed tomography for characterising the fibre orientation in unidirectional composite materials. Composites Part A: Applied Science and Manufacturing 97:83–92. https://doi.org/10.1016/j.compositesa.2016.12.028

Published online 05 January 2024

621 Emsley AM, Heywood RJ, Ali M, Eley CM (1997) On the kinetics of degradation of cellulose. Cellulose 4:1–5.
622 https://doi.org/10.1023/A:1018408515574

623 Fayolle B, Richaud E, Colin X, Verdu J (2008) Review: degradation-induced embrittlement in semi-crystalline
624 polymers having their amorphous phase in rubbery state. J Mater Sci 43:6999–7012.
625 https://doi.org/10.1007/s10853-008-3005-3

626 Fernández-Diego C, Carrascal IA, Ortiz A, et al (2021) Fracture toughness as an alternative approach to quantify
627 the ageing of insulation paper in oil. Cellulose 28:11533–11550. https://doi.org/10.1007/s10570-021-
628 04237-3

629 Ferrandin-Schoffel N, Dupont A-L, Martineau-Corcos C, Fichet O (2023) Routes to improve the strengthening
630 of paper with aminoalkylalkoxysilanes. Cellulose 30:539–556. https://doi.org/10.1007/s10570-022-
631 04906-x

632 Frase RW (1997) Preserving our Documentary Heritage: The Case for Permanent Paper. IFLA Journal 23:140–
633 143. https://doi.org/10.1177/034003529702300212

634 Gehlen MH (2010) Kinetics of autocatalytic acid hydrolysis of cellulose with crystalline and amorphous
635 fractions. Cellulose 17:245–252. https://doi.org/10.1007/s10570-009-9385-y

636 Gurnagul N, Page DH (1989) The Difference between Dry and Rewetted Zero-Span Tensile Strenght of Paper.
637 TAPPI Journal 72:164–167

638 Haas DW, Hrutfiord BF, Sarkanen KV (1967) Kinetic study on the alkaline degradation of cotton
639 hydrocellulose. J Appl Polym Sci 11:587–600. https://doi.org/10.1002/app.1967.070110408

640 Haslach, Jr. HW (2000) The Moisture and Rate-Dependent Mechanical Properties of Paper: A Review.
641 Mechanics of Time-Dependent Materials 4:169–210. https://doi.org/10.1023/A:1009833415827

642 Henniges U, Odabas N, Potthast A, Rosenau T (2016) Cellulosic fines: Properties and effects. Progress in
643 Materials Science 83:574–594. https://doi.org/10.1016/j.pmatsci.2016.07.006

644 Hill DJT, Le TT, Darveniza M, Saha T (1995) A study of degradation of cellulosic insulation materials in a
645 power transformer. Part 2: tensile strength of cellulose insulation paper. Polymer Degradation and
646 Stability 49:429–435. https://doi.org/10.1016/0141-3910(95)00100-Z

647 Hirn U, Schennach R (2015) Comprehensive analysis of individual pulp fiber bonds quantifies the mechanisms
648 of fiber bonding in paper. Sci Rep 5:10503. https://doi.org/10.1038/srep10503

649 Horst TH, Smith RD, Potthast A, Hubbe MA (2020) Accelerated Aging of Deacidified and Untreated Book
650 Paper in 1967 Compared with 52 Years of Natural Aging. Restaurator International Journal for the
651 Preservation of Library and Archival Material 41:131–152. https://doi.org/10.1515/res-2020-0006

652 Iribarne J, Schroeder LR (2000) The use of fundamental fiber properties to study pulp strenght. In: International
653 Paper Physics Seminar. Grenoble, France, p 19

654 Jeong M-J, Potthast A (2021) Improving the accuracy of estimating paper permanence for accelerated
655 degradation in closed vials. Cellulose 28:4053–4068. https://doi.org/10.1007/s10570-021-03804-y

656 Kolar J (1997) Mechanism of Autoxidative Degradation of Cellulose. Restaurator 18:163–176.
657 https://doi.org/10.1515/rest.1997.18.4.163

658 Kontturi KS, Lee K-Y, Jones MP, et al (2021) Influence of biological origin on the tensile properties of cellulose
659 nanopapers. Cellulose 28:6619–6628. https://doi.org/10.1007/s10570-021-03935-2

660 Kortschot MT (1997) The role of the fibre in the structural hierarchy of paper. In: The Fundametals of
661 Papermaking Materials, Trans. of the XIth Fund. Res. Symp. C.F. Baker, Cambridge, pp 351–399

Published online 05 January 2024

Kurei T, Hioki Y, Kose R, et al (2022) Effects of orientation and degree of polymerization on tensile properties in the cellulose sheets using hierarchical structure of wood. Cellulose 29:2885–2898. https://doi.org/10.1007/s10570-021-04160-7

l'Anson SJ, Karademir A, Sampson WW (2006) Specific Contact Area and the Tensile Strength of Paper. Appita Journal 59:11

Leheny S, Robbins TC, Robbins CK, et al (2021) Directional dependence of the mechanical properties of aged paper. Mechanics of Materials 162:104036. https://doi.org/10.1016/j.mechmat.2021.104036

Maraghechi S, Bosco E, Suiker ASJ, Hoefnagels JPM (2023) Experimental characterisation of the local mechanical behaviour of cellulose fibres: an in-situ micro-profilometry approach. Cellulose 30:4225–4245. https://doi.org/10.1007/s10570-023-05151-6

Margutti S, Conio G, Calvini P, Pedemonte E (2001) Hydrolytic and Oxidative Degradation of Paper. Restaurator 22:67–83. https://doi.org/10.1515/REST.2001.67

Marulier C, Dumont PJJ, Orgéas L, et al (2015) 3D analysis of paper microstructures at the scale of fibres and bonds. Cellulose 22:1517–1539. https://doi.org/10.1007/s10570-015-0610-6

Neimo L (1999) Papermaking chemistry, Fapet Oy. Helsinki, Finlande

Nevell TP, Zeronian SH (1985) Cellulose Chemistry and its Applications, Ellis Horwood. Chichester, UK

Page DH (1969) A theory for the tensile strenght of paper. Tappi Journal 52:674–681

Peyrega C, Jeulin D, Delisée C, Malvestio J (2009) 3D morphological modelling of a random fibrous network. Image Anal Stereol 28:129. https://doi.org/10.5566/ias.v28.p129-141

Picu CR (2021) Constitutive models for random fiber network materials: A review of current status and challenges. Mechanics Research Communications 114:103605. https://doi.org/10.1016/j.mechrescom.2020.103605

Piovesan C, Fabre-Francke I, Paris-Lacombe S, et al (2018) Strengthening naturally and artificially aged paper using polyaminoalkylalkoxysilane copolymer networks. Cellulose 25:6071–6082. https://doi.org/10.1007/s10570-018-1955-4

Potthast A, Rosenau T, Kosma P (2006) Analysis of Oxidized Functionalities in Cellulose. In: Klemm D (ed) Polysaccharides II, Springer. Berlin, Heidelberg, pp 1–48

Richely E, Bourmaud A, Placet V, et al (2022) A critical review of the ultrastructure, mechanics and modelling of flax fibres and their defects. Progress in Materials Science 124:100851. https://doi.org/10.1016/j.pmatsci.2021.100851

Sampson WW (2009) Materials properties of paper as influenced by its fibrous architecture. International Materials Reviews 54:134–156. https://doi.org/10.1179/174328009X411154

Sampson WW (2001) The structural characterisation of fibre networks in papermaking processes—a review. In: Baker CF (ed) The Science of Papermaking, FRC. Manchester, pp 1205–1288

Sampson WW (2003) The statistical geometry of fractional contact area in random fibre networks. Journal of pulp and paper science 29:412–416

Sampson WW, Wang D (2020) A model for roughness statistics of heterogeneous fibrous materials. J Mater Sci 55:2636–2644. https://doi.org/10.1007/s10853-019-04193-1

Schmied FJ, Teichert C, Kappel L, et al (2012) Joint strength measurements of individual fiber-fiber bonds: An atomic force microscopy based method. Review of Scientific Instruments 83:073902. https://doi.org/10.1063/1.4731010

Published online 05 January 2024

SriBala G, Vinu R (2014) Unified Kinetic Model for Cellulose Deconstruction via Acid Hydrolysis. Ind Eng Chem Res 53:8714–8725. https://doi.org/10.1021/ie5007905

Stephens CH, Whitmore PM, Morris HR, Bier ME (2008) Hydrolysis of the Amorphous Cellulose in Cotton-Based Paper. Biomacromolecules 9:1093–1099. https://doi.org/10.1021/bm800049w

Strlič M, Kolar J (eds) (2005) Ageing and stabilisation of paper, National and University Library. Ljubljana

Syerko E, Comas-Cardona S, Binetruy C (2012) Models of mechanical properties/behavior of dry fibrous materials at various scales in bending and tension: A review. Composites Part A: Applied Science and Manufacturing 43:1365–1388. https://doi.org/10.1016/j.compositesa.2012.03.012

Tétreault J, Bégin P, Paris-Lacombe S, Dupont A-L (2019) Modelling considerations for the degradation of cellulosic paper. Cellulose 26:2013–2033. https://doi.org/10.1007/s10570-018-2156-x

Vibert C, Fayolle B, Ricard D, Dupont A-L (2023) Decoupling hydrolysis and oxidation of cellulose in permanent paper aged under atmospheric conditions. Carbohydrate Polymers 120727. https://doi.org/10.1016/j.carbpol.2023.120727

Wathén R, Batchelor W, Westerlind B, Niskanen K (2005) Analysis of strains in the fracture process zone. Nordic Pulp & Paper Research Journal 20:392–398. https://doi.org/10.3183/npprj-2005-20-04-p392-398

Wernersson ELG, Borgefors G, Borodulina S, Kulachenko A (2014) Characterisations of fibre networks in paper using micro computed tomography images. Nordic Pulp & Paper Research Journal 29:468–475. https://doi.org/10.3183/npprj-2014-29-03-p468-475

Whitmore PM, Bogaard J (1995) The Effect of Oxidation on the Subsequent Oven Aging of Filter Paper. Restaurator 16:10–30. https://doi.org/10.1515/rest.1995.16.1.10

Wilson WK, Harvey JL, Mandel J, Worksman T (1955) Accelerated Aging of Record Papers Compared with Normal Aging. TAPPI Journal 38:543–548

Young RA, Rowell RM (1986) Cellulose. Structure, Modification and Hydrolysis, John Wiley&Sons Inc

Yue H, Rubalcaba JC, Cui Y, et al (2019) Determination of cross-sectional area of natural plant fibres and fibre failure analysis by in situ SEM observation during microtensile tests. Cellulose 26:4693–4706. https://doi.org/10.1007/s10570-019-02428-7

Zervos S, Moropoulou A (2005) Cotton Cellulose Ageing in Sealed Vessels. Kinetic Model of Autocatalytic Depolymerization. Cellulose 12:485–496. https://doi.org/10.1007/s10570-005-7131-7

Zou X, Gurnagul N, Uesaka T (1993) The role of lignin in the mechanical permanence of Paper - Part I: Effect of lignin content. Journal of pulp and paper science 19:235–239

Zou X, Gurnagul N, Uesaka T, Bouchard J (1994) Accelerated aging of papers of pure cellulose: mechanism of cellulose degradation and paper embrittlement. Polymer Degradation and Stability 43:393–402. https://doi.org/10.1016/0141-3910(94)90011-6

Supplementary Information

The online version contains supplementary material: https://doi.org/10.1007/s10570-023-05683-x.

Published online 05 January 2024